Cancer Immunology, Immunotherapy (2025) 74:145
https://doi.org/10.1007/s00262-025-03992-7

RESEARCH

Neoantigen-based mRNA vaccine exhibits superior anti-tumor activity compared to synthetic long peptides in an in vivo lung carcinoma model

Cao Minh Nguyen[1] · Trung T. Vu[1] · Minh Nguyen Nguyen[1] · Thao-Suong Tran-Nguyen[1] · Chi Thien Huynh[2] · Quang Thanh Ha[2] · Hoai-Nghia Nguyen[1] · Le Son Tran[1]

Received: 27 October 2024 / Accepted: 21 February 2025 / Published online: 12 March 2025
© The Author(s) 2025

Abstract

Neoantigen vaccines hold great promise in cancer immunotherapy, but the comparative efficacy of different vaccine platforms, particularly in the context of tumor burden (TB), remains insufficiently studied. In this research, we evaluated the safety and therapeutic efficacy of synthetic long peptide and mRNA-based vaccines, both designed to target identical neoantigens across different Lewis Lung Carcinoma (LLC) tumor burdens. We employed the LLC syngeneic mouse model, a widely used preclinical model for aggressive and immunosuppressive tumors. Our findings demonstrated that the mRNA-based vaccine significantly outperformed the peptide-based vaccine in preventing tumor growth in mice with low TB. These results underscore the potential of mRNA vaccines as a more effective approach for treating aggressive tumors, contributing valuable insights for the future development of neoantigen-based cancer vaccines.

Keywords Lewis lung carcinoma · Neoantigen · Synthetic long peptide vaccine · mRNA-based vaccine · mRNA-LNPs · Cancer immunotherapy

Introduction

Cancer immunotherapy leverages the immune system to fight cancer by enhancing its ability to target cancer cells. Tumor-associated antigens (TAAs) and tumor-specific antigens (TSAs) are key immunotherapy targets, as they are presented on tumor cell membranes [1]. TAA-targeted therapies have shown success but risk autoimmunity due to expression in normal cells [2]. TSAs, however, are mutation-derived and tumor-specific, making TSA-based therapies, particularly synthetic peptide vaccines, a promising option. Peptide vaccines offer safety, specificity, and ease of production, though they require high doses, strong adjuvants, effective delivery, and sustained presence in the body [3, 4].

Recently, mRNA vaccines have emerged as a compelling alternative to TSA peptide vaccines. The mRNA-lipid nanoparticle (LNP) platform effectively addresses many issues associated with peptide vaccines by offering easier delivery, self-adjuvating properties, extended duration, and increased TSA production [5, 6]. Numerous studies have explored the application of TSAs in both peptide and mRNA vaccine formats to inhibit tumor growth, yielding significant results [7, 8]. In the NCT03480152 study, personalized tumor-specific antigens (TSAs) derived from mutations in *TP53*, *KRAS*, and *PIK3CA* were used to develop tandem minigene (TMG) mRNA vaccines for patients with metastatic gastrointestinal cancer [9]. The vaccines were well-tolerated and generated strong T cell responses but did not result in tumor shrinkage. Despite the promise of these vaccines, the specific contexts in which they can successfully counteract the immunosuppressive strategies employed by tumors remain poorly understood [10]. In this study, we investigate these dynamics using the Lewis lung carcinoma (LLC) syngeneic mouse model, a notoriously difficult-to-treat cancer model [11], to evaluate the immunogenicity and anti-tumor efficacy of TSA-targeted peptide and mRNA vaccines (Fig. 1).

The LLC mouse model is particularly informative for studying tumor immune evasion, as it exhibits a variety of

✉ Le Son Tran
leson1808@gmail.com

[1] Medical Genetics Institute, Ho Chi Minh City, Vietnam

[2] Biotechnology Center of Ho Chi Minh City, Ho Chi Minh City, Vietnam

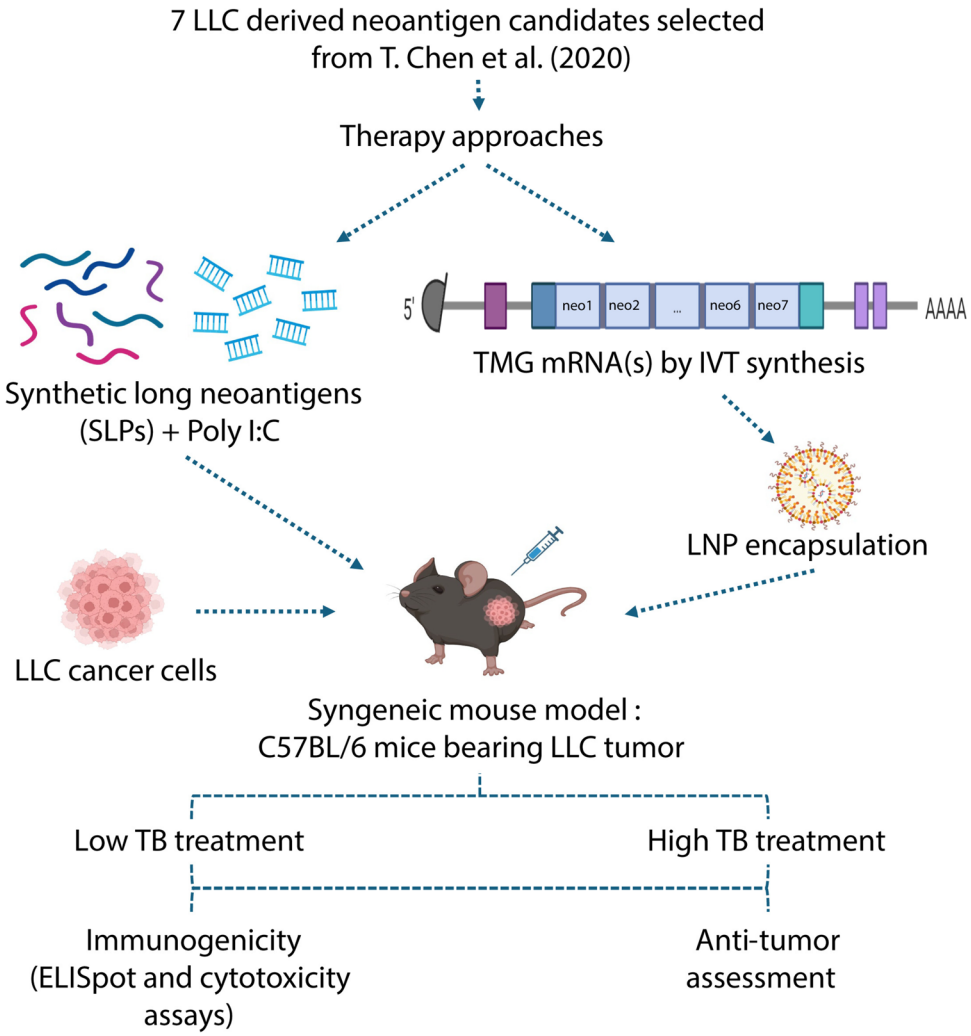

Fig. 1 Schematic Diagram: Testing Two Vaccination Approaches as Therapy in LLC Syngeneic C57BL/6 Mice. Seven neoantigen candidates, identified from a published study, were selected and used as antigens in two therapy approaches: SLP vaccine and mRNA vaccine. These approaches were applied in LLC syngeneic C57BL/6 mouse models with either low or high TB. Immunogenicity and immune response against these vaccines were evaluated using ELISpot and cytotoxicity assays, while the efficacy of the vaccination approaches was assessed by monitoring tumor development

mechanisms that impede the body's immune system. These mechanisms include the downregulation of major histocompatibility complex (MHC) class I and II molecules [12, 13], which are crucial for antigen presentation and recognition by T cells. Additionally, LLC tumors secrete immunosuppressive cytokines that further inhibit immune activation [14]. They also promote the expansion of T-regulatory cells (Tregs) and myeloid-derived suppressor cells (MDSCs) [14], both of which play significant roles in dampening immune responses. Moreover, the LLC tumor microenvironment presents physical barriers that make immune cell infiltration challenging, compounding the difficulty of effectively targeting and eliminating the tumor [11]. Given these complexities, the LLC mouse model provides an ideal platform for assessing the potential of synthetic long peptides (SLPs) and mRNA-based vaccines that target multiple neoantigens. By using this model, we aim to elucidate the immunological mechanisms at play and determine the efficacy of these vaccine approaches in overcoming the multifaceted immunosuppressive environment characteristic of LLC tumors.

Materials and methods

Cell lines and mice

The Lewis lung carcinoma (LLC1) cell line (CRL-1642) was obtained from ATCC and cultured in Dulbecco's Modified Eagle Medium (DMEM; GIBCO, USA) supplemented with 10% fetal bovine serum (GIBCO, USA) and 1% penicillin–streptomycin (P/S; GIBCO, USA). Male C57BL/6 mice, aged 6–8 weeks, were purchased from BioLASCO Taiwan Co., Ltd.

Synthetic peptides

The 24-mer wild-type and mutant peptide sequences were obtained from a previous study [15] and synthesized by GenScript Biotech (USA) with a purity of ≥ 98% (Table 1).

Table 1 Adapted from the paper 15, this table provides details of the seven mutant peptides and the wild-type peptides analyzed in this study. Mutated amino acids in each peptide are highlighted in bold. These sequences were used to design mutant mRNA and wild-type mRNA vaccines. The table also includes the variant allele frequency (VAF) of each peptide, along with MHC I and MHC II binding predictions. Binding scores below 3 are considered indicative of strong MHC binding. Three peptides could not be synthesized: 1, 3, and 8

Peptide from paper	Peptide used in this study	Mutation peptide	Wild-type peptide	VAF (mutation read/wildtype read)	Classify	MHCI, H2-D	MHCI, H2-K	MHCII, H2-A
Pep 1	Unable to synthesize	KPFYPALISYM**G**SGPVVAMVWEGP	KPFYPALISYM**S**SGPVVAMVWEGP	7%	heterozygosity		0.42	0.2
Pep 2	Neo1	QIKGKDSFLYSLPH**S**HPVNAACFS	QIKGKDSFLYSLPH**R**HPVNAACFS	36%	heterozygosity	0.13	2.1	0.45
Pep 3	Unable to synthesize	KVLGFLFFV**T**AYFLYKSPSVSSDG	KVLGFLFFV**A**AYFLYKSPSVSSDG	75%	heterozygosity	2.5	0.59	0.49
Pep 4	Neo2	KKHKKEKAV**S**IATPATAAPAAVSA	KKHKKEKAV**T**IATPATAAPAAVSA	100%	homozygosity	2.4		0.59
Pep 5	Neo3	ELELALSPIH**Y**SSAIPAAGSNQVT	ELELALSPIH**D**SSAIPAAGSNQVT	20%	heterozygosity	2.7	1.75	0.78
Pep 6	Neo4	PEHYVDYTY**I**ATKLWAGPDPSSPT	PEHYVDYTY**M**ATKLWAGPDPSSPT	100%	homozygosity	2.3	0.61	0.89
Pep 7	Neo5	LVSSRSHVWPAPLP**L**LQHGCEKGG	LVSSRSHVWPAPLP**W**LQHGCEKGG	50%	heterozygosity		0.62	1.34
Pep 8	Unable to synthesize	VMTFEDFAAQVFSPSPSYS**L**SGTD	VMTFEDFAAQVFSPSPSYS**V**SGTD	38%	heterozygosity	1.3		1.89
Pep 9	Neo6	GPQAISKAT**F**ETLAADPTPAATIV	GPQAISKAT**S**ETLAADPTPAATIV	43%	heterozygosity		1.95	1.98
Pep 10	Neo7	QLLNGHAPAAGPNL**S**GLPQANRHH	QLLNGHAPAAGPNL**A**GLPQANRHH	100%	homozygosity	1		2.53

Syngeneic tumor mouse model

C57BL/6 mice were inoculated subcutaneously with either 50,000 (low TB) or 500,000 LLC cells (high TB) in the right flank. Tumor growth and body weight were monitored every two days, with tumor volumes measured using calipers and calculated as $(A \times B^2) \times 0.5$ (A = length, B = width). Treatments began on day 14, when 80% of high TB mice had developed tumors, and on day 14 for low TB mice regardless of tumor presence (as tumors were often not detectable at this time in the low TB group). Treatments were administered every seven days. The study endpoint was defined as tumor volumes reaching 3000 mm^3. Animal experimentation was approved by the Animal Ethics Committee A at the University of Science in Ho Chi Minh City, Vietnam (permit number 562/KHTN-ACUCUS), and mice were euthanized via CO_2 inhalation.

For peptide vaccination, three different peptide formulations were used. One formulation contained a mixture of seven peptides at 14 µg/peptide, another consisted of three peptides at 33 µg/peptide, and the third included a single peptide at 100 µg. Each formulation was mixed with 50 µg of polyinosinic:polycytidylic acid (poly(I:C)) in PBS, prepared in a total volume of 100 µL, and injected subcutaneously into the right flank.

For mRNA vaccination, mRNA-LNPs were administered intravenously (IV) into the tail vein and intramuscularly (IM) into the left hind limb, with each site receiving 1.5 µg of mRNA in a 100 µL volume.

IFN-γ ELISpot assay

ELISpot assay was conducted using the ELISpot Plus: Mouse IFN-γ (HRP) Kit (3321-4HST, Mabtech, Sweden) as per the manufacturer's instructions. Seven days after the final injection, mice were sacrificed, and splenocytes were isolated and rested for 48 h before the assay. The culture medium consisted of RPMI 1640 (GIBCO, USA) with 10% FBS, 1% penicillin–streptomycin, 10 µM HEPES, 50 µM 2-mercaptoethanol, and 20 ng/mL murine IL-2. For the assay, a single SLP at 40 µg/mL was co-cultured with 200,000 splenocytes in 200 µL of medium in a round bottom 96-well plate, incubated at 37 °C for 24 h. After refreshing the medium, cells were transferred to ELISpot plates and incubated for an additional 24 h. Concanavalin A (Invitrogen, USA), diluted 1:500, served as a positive control. Cytokine secretion was detected according to the manufacturer's instructions, and spot forming units (SFU) were counted using an ASTOR 2 reader (Mabtech, Sweden). Negative control wells, containing no peptides, were used to normalize SFU values in peptide-pulsed wells. We chose to normalize the ELISpot data to the responses induced by the WT peptide to account for baseline T cell activation. This normalization method enables a clearer assessment of the mutant-specific immune responses by highlighting differences attributable specifically to mutant peptide stimulation.

Intracellular cytokine staining (ICS)

ICS was performed using the BD Cytofix/Cytoperm Plus Kit (555,028, BD Biosciences, USA) following the manufacturer's protocol. Splenocytes from the ELISpot assay were transferred to U-bottom 96-well plates and incubated with BD GolgiPlug (1:1000 dilution) for 8 h at 37 °C. Afterward, the cells were washed with PBS, and Fc receptors were blocked using TruStain FcX PLUS (anti-mouse CD16/32) antibody (156,604, BioLegend, USA) for 15 min. The cells were then fixed, permeabilized, and stained with antibodies as per the kit instructions. After staining with PerCP/Cyanine5.5 anti-mouse CD3, PE anti-mouse CD8a, APC anti-mouse CD4, and FITC anti-mouse IFN-γ antibodies (all at 1:100 dilution), the cells were incubated overnight at 4 °C in the dark, washed, and resuspended in PBS for analysis on a NovoCyte Advanteon Flow Cytometer (Agilent, USA).

mRNA construction and production

To construct the mRNA, seven mutated peptides (Table 1) were linked using the GGSGGGGSGG linker to form a tandem minigene. A signal peptide sequence (MRVTAPRTLILLLSGALALTETWAGS) was added to the 3' end of the minigene using the same linker. An MITD sequence (IVGIVAGLAVLAVVVIGAVVATVMCRRKSSGGKGGSYSQAASSDSAQG-SDVSLTA) was linked to the 5' end with a GGSLGGGGSG linker. The complete insert was reverse-translated into RNA and codon-optimized (IDT, USA), with two stop codons (TGA TGA) added at the 5' end. The mRNA backbone was derived from previous work, with the modified T7 promoter and 3' UTR added to the 3' end, and the 5' UTR, poly(A) tail, and a BspQI restriction site included at the 5' end.

The full mRNA construct was cloned into a high-copy plasmid synthesized by Epoch Life Science (USA), transformed into NEB Turbo Competent *E. coli* (New England Biolabs, UK), grown for plasmid extraction, and linearized using BspQI (New England Biolabs, UK). In vitro transcription (IVT) was performed using the HiScribe T7 mRNA Kit with CleanCap Reagent AG (New England Biolabs, UK), supplemented with 1 U/µL RNase inhibitor and 0.002 U/µL pyrophosphatase (New England Biolabs, UK). To minimize innate immune responses, N1-Methylpseudouridine 5'-Triphosphate (TriLink, USA) replaced UTP in the IVT reaction. A similar process was used to create the wild-type plasmid and corresponding mRNA based on the wild-type peptide.

mRNA purification by HPLC

Following synthesis, the mRNA was analyzed using 2% agarose gel electrophoresis and purified by high-performance liquid chromatography (HPLC). It was then concentrated using an Amicon Ultra Centrifugal Filter (30 kDa MWCO, Millipore, USA) to remove double-stranded RNA (dsRNA) and truncated molecules, as described by Karikó et al. (2011) [16]. A temperature of 55 °C was used for optimal results.

Dot blot analysis

The purified mRNA was tested for dsRNA contamination using a dot blot assay. Briefly, 100 ng of mRNA was blotted onto a Nytran SuPerCharge membrane (Cytiva, USA), dried, and blocked with 5% non-fat milk in TBS-T buffer (0.05% Tween-20). The membrane was incubated with a dsRNA-specific monoclonal antibody (J2) (RNT-SCI-10010200, Jena Bioscience, Germany) at a 1:100 dilution for 3 h. After washing, it was incubated with Alexa Fluor 488-conjugated goat anti-mouse secondary antibody (A32723, Thermo Fisher Scientific, USA) for 30 min and visualized using the iBright Imaging System.

LNP encapsulation

Lipid ALC-0315 (Sinopeg, China), DSPC (Merck, Germany), cholesterol (Merck, Germany), and ALC-0159 (Sinopeg, China) were dissolved in ethanol at 10 mM and mixed in a molar ratio of 46.3:9.4:42.7:1.6. Purified mRNA was diluted in acetate buffer (5.67 mM sodium acetate, 19.33 mM acetic acid, pH 4.0) to a concentration of 113.18 ng/µL. Lipid and mRNA solutions were combined using NanoAssemblr Benchtop cartridges (Precision NanoSystems, Canada), with flow rates of 2 mL/min for lipids and 6 mL/min for mRNA, achieving an N/P ratio of 6. The mRNA-LNP complex was collected and dialyzed overnight against PBS using SnakeSkin Dialysis Tubing, 10 K MWCO (Thermo Fisher Scientific, USA). Nanoparticle size was measured using a Nanoparticle Analyzer (Horiba, Japan), and encapsulation efficiency was determined using the RiboGreen assay (Thermo Fisher Scientific, USA) as described [17].

For DiR staining, DiR (D12731, Thermo Fisher Scientific, USA) was added to the LNP at a concentration of 1% before mixing with mRNA and injected intravenously into the mice. The distribution was detected using the IVIS imaging system (Revvity, USA).

Cytotoxicity assay

LLC1 cells were stained with CellTrace CFSE (C34554, Thermo Fisher Scientific, USA) and seeded into U-bottom 96-well plates at a density of 1,000 cells per well in RPMI 1640 medium supplemented with 10% FBS. After 24 h, SLPs (40 µg/mL) were added to each well and incubated for an additional 12 h. Following peptide incubation, the medium was replaced, and splenocytes were added at varying ratios (2:1, 5:1, and 10:1 splenocytes to LLC1 cells). After 8 h of incubation, the cells were washed twice with PBS and stained with Zombie Red viability dye (423,110, BioLegend, USA), diluted 1:500 in PBS for 20 min at room temperature (RT) to detect dead cells. After staining, the cells were washed with PBS containing 5% FBS to stop the Zombie Red reaction, trypsinized, washed with PBS, and resuspended in 100 µL of PBS. The samples were then analyzed by flow cytometry using the NovoCyte Advanteon Flow Cytometer (Agilent, USA). The number of dead cells was determined by subtracting the percentage of CFSE + Zombie + cells from the percentage of CFSE + Zombie– cells.

Results

Neoantigen-based SLPs show limited anti-tumor activity

While neoantigen vaccination using SLPs holds promise for inducing strong anti-tumor immune responses, its clinical application has faced limited success [18]. To evaluate its efficacy, we vaccinated two groups of LLC-bearing C57BL/6 mice with a mixture of seven SLPs (Table 1), containing either LLC-specific mutations previously shown to induce neoantigen-specific immunity in tumor-naive mice or corresponding wild-type peptides [15]. One group had low TB, while the other had high TB (Fig. 2A). Since tumor size prior to treatment varied among animals in the high TB model, we randomized the treatment groups to ensure a similar total TB across all groups at the start of the experiment (Fig. S1). In both cases, SLP-vaccinated mice demonstrated a favorable safety profile, with no significant changes in body weight or blood protein levels compared to mice treated with the adjuvant poly IC alone (Fig. S2).

We observed no significant differences in tumor volumes (Fig. 2B–E) or survival rates (Fig. S3A and S3B) between mice treated with mutant SLPs and those treated with wild-type SLPs under both conditions. These findings indicate that peptide-based vaccines demonstrated limited anti-tumor efficacy against LLC tumors. Next, we evaluated whether tumor-bearing mice generated immune responses to mutant

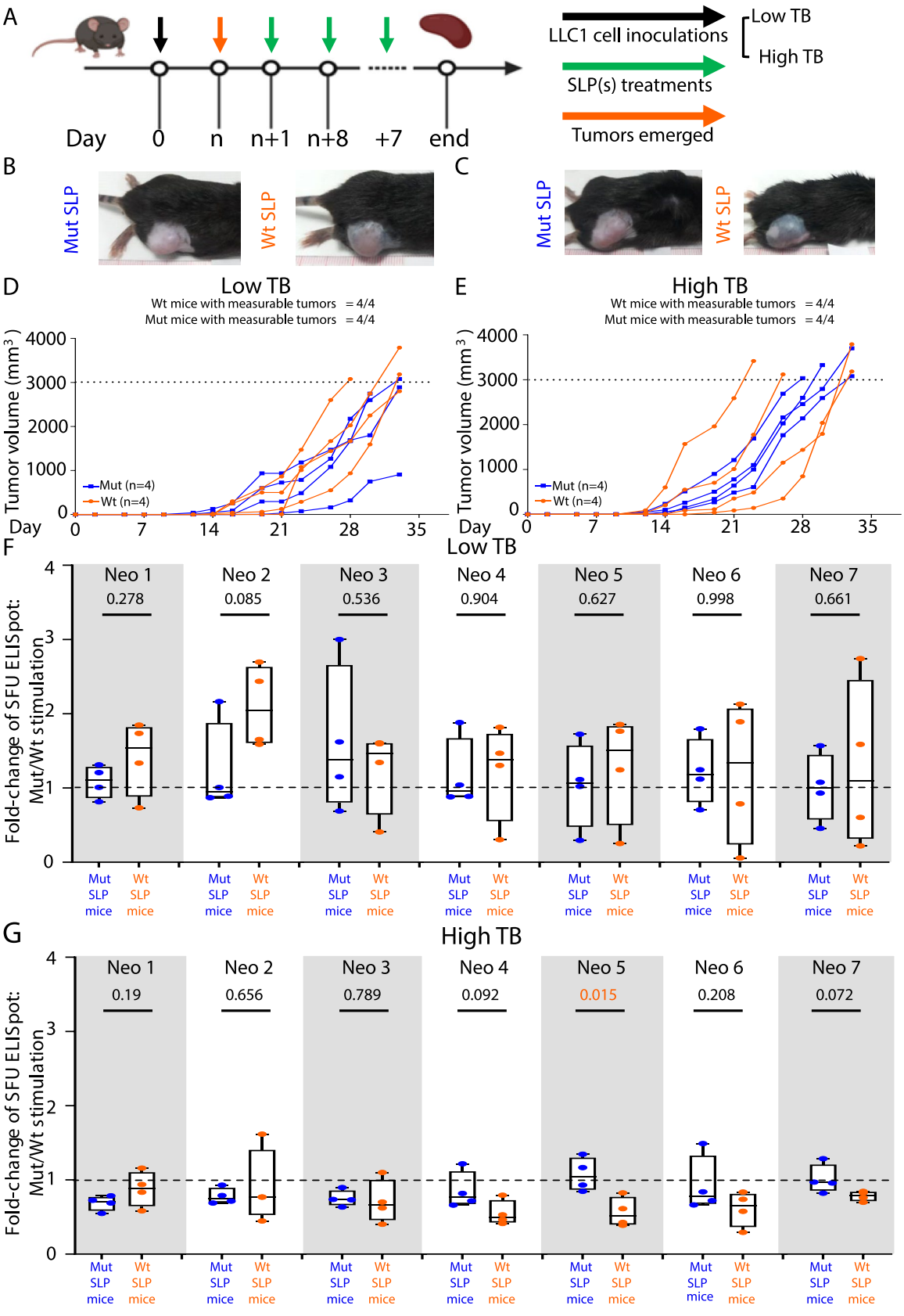
A
Day 0 n n+1 n+8 +7 end
LLC1 cell inoculations
Low TB
High TB
SLP(s) treatments
Tumors emerged
B
Mut SLP
Wt SLP
C
Mut SLP
Wt SLP
D
Low TB
Wt mice with measurable tumors = 4/4
Mut mice with measurable tumors = 4/4
Tumor volume (mm3)
Mut (n=4)
Wt (n=4)
Day
E
High TB
Wt mice with measurable tumors = 4/4
Mut mice with measurable tumors = 4/4
Tumor volume (mm3)
Mut (n=4)
Wt (n=4)
Day
F
Low TB
Neo 1 0.278
Neo 2 0.085
Neo 3 0.536
Neo 4 0.904
Neo 5 0.627
Neo 6 0.998
Neo 7 0.661
Fold-change of SFU ELISpot: Mut/Wt stimulation
Mut SLP mice
Wt SLP mice
G
High TB
Neo 1 0.19
Neo 2 0.656
Neo 3 0.789
Neo 4 0.092
Neo 5 0.015
Neo 6 0.208
Neo 7 0.072
Fold-change of SFU ELISpot: Mut/Wt stimulation
Mut SLP mice
Wt SLP mice

◂**Fig. 2** SLPs demonstrate very limited anti-tumor activity in LLC syngeneic C57BL/6 mice. **A** Experimental design to test the therapeutic effect of SLP vaccines on LLC-bearing C57BL/6 mice. **B**, **C** Representative images of tumor on day 30 under low (**B**) or high TB (**C**). **D**, **E** Tumor development in LLC-bearing mice injected with wild-type or mutant SLP vaccines under low (**D**) and high tumor burden (**E**). **F**, **G** IFN-γ production was measured by ELISpot in splenocytes from vaccinated mice under low (**F**) and high TB (**G**) after stimulation with wild-type (Wt) and mutant (Mut) peptides. Individual data point represents the fold change in the number of ELISpot spots in Mut peptide-activated splenocytes relative to the corresponding Wt-activated splenocytes for each individual mouse. Mean ± SEM is shown. ns: not significant, $*p < 0.05$, $**p < 0.01$, $***p < 0.001$ (independent (unpaired) two-sample t test)

SLP peptides by measuring ex vivo IFN-γ production in splenocytes from mice vaccinated with either wild-type or mutant SLPs. At baseline, no significant differences in IFN-γ production were observed between the two groups under both low and high TB conditions (Fig. S3C and S3D). We then performed in vitro stimulation using individual mutant SLPs and their corresponding wild-type peptides. After normalizing IFN-γ levels to wild-type SLP stimulation, we observed sporadic recall responses (fold change > 1) to the seven tested mutant peptides in splenocytes from mutant SLP-vaccinated mice or de novo response in splenocytes in wild-type SLP-vaccinated mice under low TB condition (Figs. 2F and S4A). However, no IFN-γ induction was observed in any vaccinated mice under high tumor burden (fold change < 1, Figs. 2G and S4B). Importantly, no significant differences in IFN-γ induction were observed between the two groups of splenocytes following stimulation with all seven tested mutant peptides under both conditions (Figs. 2F, G, S4A and S4B). These results suggest that neoantigen vaccination with SLPs elicited ineffective mutation-specific immune responses in LLC-bearing mice, regardless of TB.

To strengthen our findings, we examined various regimens for the SLP vaccines, including treatment schedules, dosages, and peptide components. We first assessed the timing of vaccination by injecting low TB mice with the 7-peptide pool vaccine (14 μg per peptide) at an earlier time point (day 7). We observed slower tumor growth in low TB mice vaccinated on day 7, suggesting that the innate immune response during early treatment may contribute to tumor growth suppression (Fig. S5A). However, similar to the treatment on day 14 (Fig. 2D), no significant differences were observed between wild-type peptide- and mutant peptide-treated mice (Fig. S5A). To increase the doses of peptides with confirmed immunogenicity while adhering to the overall maximal dose of a vaccine pool, as required by ethical regulations, we generated alternative peptide pools. These included 3-peptide pools containing three immunogenic peptides (Neo1, Neo3, and Neo4; Fig. S5B) at double the dose (33 μg per peptide) at two time points: day 7 (Fig. S5B) and day 14 (Fig. S5C). We also tested single-peptide pools containing individual immunogenic peptides at sevenfold higher doses (100 μg per peptide) on day 7 (Fig. S5D–S5F). Across all these settings, we observed no significant differences in tumor growth between mutant peptide- and wild-type peptide-treated mice.

Development of a mRNA-LNP platform for mRNA vaccination

Due to the limited efficacy of neoantigen peptide vaccines and promising results from mRNA cancer vaccine trials [19], we developed an mRNA-LNP platform as an alternative. This platform delivers mRNA encoding multiple neoantigens encapsulated in LNPs for in vivo vaccination.

We first performed IVT to generate neo-mRNA encoding 7 different neoantigens or 7 different corresponding wild-type peptides (WT mRNA), linked by the GGSGGGGSGG linker and flanked by 5'UTR and 3'UTR sequences, including a poly-A tail (Fig. 1). The resulting neo-mRNA and WT mRNA products had the expected length of 1298 bp with high integrity (Fig. 3A). To remove dsRNA, we purified the mRNA using HPLC, as described in the method section [16]. This yielded purified mRNA in the F1 fraction (Fig. 3B), which exhibited a threefold reduction in dsRNA content, while the discarded F2 fraction showed an enrichment of dsRNA (Fig. 3C and 3D). These results confirm the successful generation of neo-mRNA and WT mRNA with low dsRNA levels. To prevent degradation in vivo, we encapsulated the purified neo-mRNA and WT mRNA into LNPs using a previously described formulation [20]. A dynamic light scattering assay showed comparable size distributions between the neo-mRNA-LNPs and WT mRNA-LNPs, with the majority of particles ranging from 90 to 150 nm, which supports cellular uptake (Fig. 3E). Additionally, a RiboGreen assay confirmed encapsulation efficiency, with an average of 80%, indicating that most of the mRNA was protected by the LNPs (Fig. 3F).

Neo-mRNA vaccine induces neoantigen-specific responses in tumor-naive mice

Next, we examined the biodistribution of mRNA-LNPs in mice following intravenous (i.v.) injection of varying doses of DIR-labeled mRNA-LNPs (Fig. 4A). The majority of the mRNA-LNPs accumulated in the liver and spleen in a dose-dependent manner (Fig. 4B and 4C). To evaluate the ability of mRNA-LNPs to induce neoantigen-specific immune responses, we measured IFN-γ production after stimulating splenocytes collected from neo-mRNA-LNP or WT mRNA-LNP vaccinated mice with either mutant or wild-type peptides. Splenocytes from neo-mRNA-LNP-vaccinated mice exhibited recall responses to all seven mutant peptides,

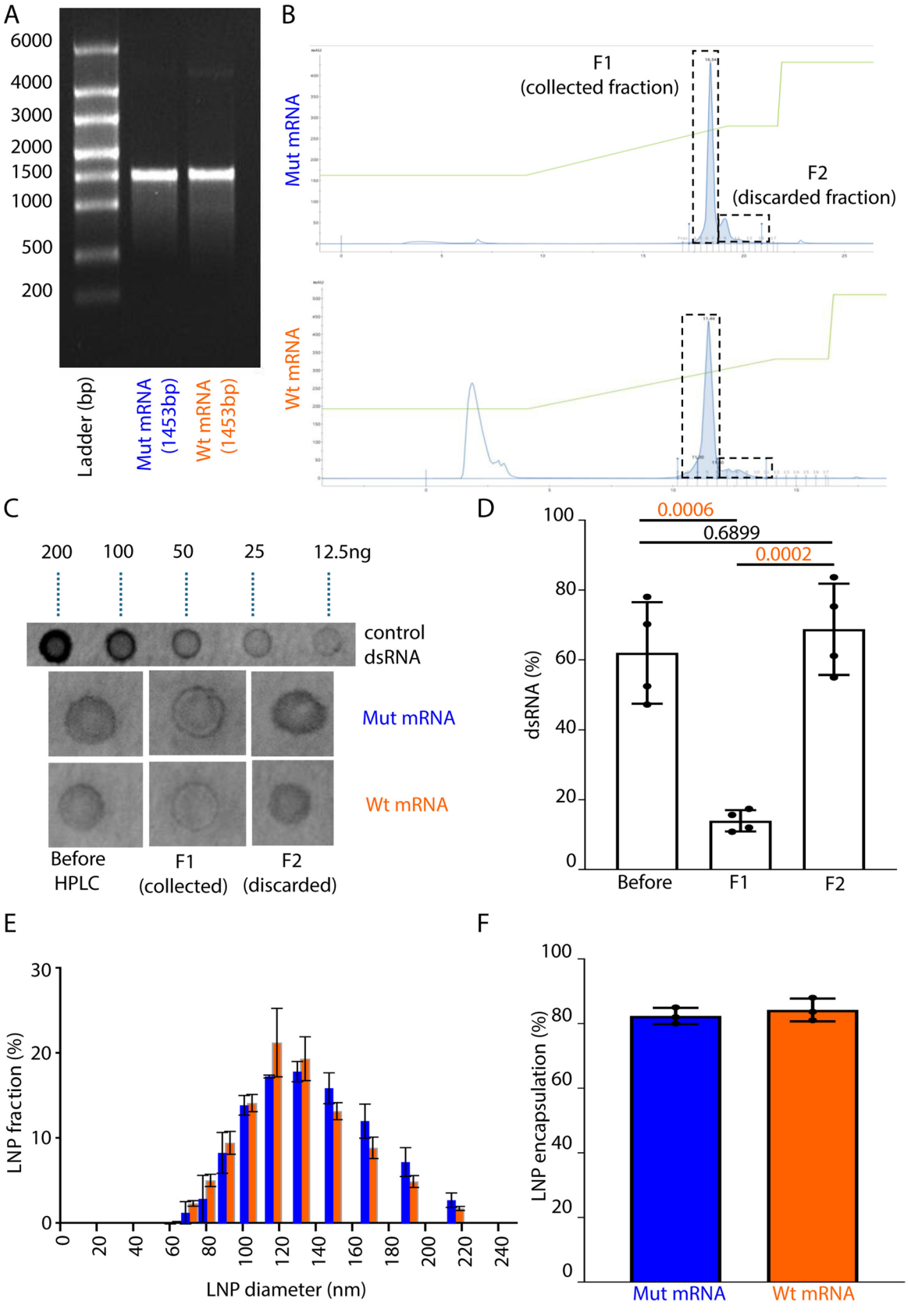
A
6000
4000
3000
2000
1500
1000
500
200
Ladder (bp)
Mut mRNA (1453bp)
Wt mRNA (1453bp)
B
Mut mRNA
F1 (collected fraction)
F2 (discarded fraction)
Wt mRNA
C
200 100 50 25 12.5ng
control dsRNA
Mut mRNA
Wt mRNA
Before HPLC
F1 (collected)
F2 (discarded)
D
0.0006
0.6899
0.0002
dsRNA (%)
Before
F1
F2
E
LNP fraction (%)
LNP diameter (nm)
F
LNP encapsulation (%)
Mut mRNA
Wt mRNA

◂**Fig. 3** Production and quality control procedures for mRNA-LNPs. **A** RNA integrity assessment by agarose gel electrophoresis. **B** HPLC purification of single-stranded mRNA to remove dsRNA. After purification, F1 was collected and F2 was discarded. **C** Detection of contaminated dsRNA before and after HPLC purification using dot blot. Different fractions of Mut mRNA (blue) and Wt mRNA (orange) were blotted and analyzed for dsRNA using an anti-dsRNA antibody. Before purification, fraction F1 (collected) and fraction F2 (discarded) were tested. **D** Quantification of contaminated dsRNA before and after HPLC purification using dot blot. Each dot presents the dsRNA concentration of each fractions (before purification, collected fraction F1 and discarded fraction F2) after compare with the standard control dsRNA to define the concentration of the dsRNA. One-way ANOVA, Šídák's multiple comparisons test). **E** mRNA-LNP size distribution analysis was performed, each column presents the fraction for size of LNP in the mRNA-LNP mixture for both Mut mRNA-LNP (blue) and Wt mRNA-LNP (orange). Mean ± SEM is shown. ns: not significant, $*p < 0.05$, $**p < 0.01$, $***p < 0.001$ (independent (unpaired) two-sample t test). F. mRNA-LNP encapsulation efficiency analysis was performed using Ribo-green assay, each dot presents the fraction of mRNA encapsulated inside the LNP particle for Mut mRNA-LNP (blue) and Wt mRNA-LNP (orange)

with IFN-γ fold changes > 1 relative to their corresponding wild-type peptides (Fig. 4D). Importantly, these responses were significantly higher than those observed in splenocytes from WT mRNA-LNP-vaccinated mice, which showed no IFN-γ induction upon stimulation with the mutant peptides (Fig. 4D). These findings demonstrate the successful generation of neo-mRNA and WT mRNA encapsulated in LNPs, which effectively deliver neoantigens to lymphoid organs and induce neoantigen-specific immune responses.

Neo-mRNA vaccines induces neoantigen-specific anti-tumor immunity in mice with low TB

To evaluate the efficacy of the mRNA vaccine in vivo, we vaccinated mice with low and high TB using either neo-mRNA-LNPs or WT mRNA-LNPs, following a similar approach to that used for peptide vaccines (Fig. 5A). Consistent with results from peptide-vaccinated mice, mRNA-vaccinated mice displayed no noticeable safety concerns or pathological phenotypes (Fig. S6). We observed a comparable biodistribution of LNPs in tumor-bearing mice compared to naïve mice, with the majority of LNPs accumulating in the liver. Notably, we also observed LNP accumulation in the tumors of tumor-bearing mice (Fig. S7 and S8).

In the low TB group, all six WT mRNA-vaccinated mice developed tumors, with two succumbing to the disease. In contrast, five out of six neo-mRNA-vaccinated mice showed no significant tumor development, with only one mouse developing a small tumor by day 35 (Fig. 5B–D). Neo-mRNA-vaccinated mice also demonstrated better survival rates compared to those vaccinated with WT mRNA (Fig. S9A). However, in the high TB group, there were no significant differences in tumor volume (Fig. 5C–E), incidence (Fig. 5E), or survival rates (Fig. S9B) between the two groups.

Next, we assessed the immune responses to the tested neoantigens in tumor-bearing mice under both low and high TB conditions. Consistent with the SLP vaccination results, no significant difference in baseline IFN-γ production was observed between splenocytes from WT- and neo-mRNA-vaccinated mice under both low and high TB conditions (Figs. S9C and S9D). However, upon in vitro stimulation with mutant or wild-type peptides, significant IFN-γ induction (fold change > 1) was detected in splenocytes from neo-mRNA-vaccinated mice when stimulated with mutant peptides 1, 3, and 4 under low TB conditions, compared to their corresponding wild-type peptides (Figs. 5F, S10, and S11A). Importantly, these induction levels were significantly higher than those observed in splenocytes from WT-vaccinated mice, which did not exhibit any significant IFN-γ induction (Figs. 5F and S11A). In contrast, high TB mice did not exhibit significant neoantigen-specific immune response after in vitro stimulation with each of the seven peptides (Fig. 5G and S11B). These findings suggest that neo-mRNA vaccination can induce neoantigen-specific IFN-γ responses and anti-tumor immunity in low TB mice but fails to do so in high TB mice.

We next performed intracellular staining using flow cytometry to determine whether the enhanced IFN-γ production observed in splenocytes from mutant mRNA-treated mice under low TB condition originated from activated $CD4^+$ or $CD8^+$ cells. Splenocytes from mutant and wild-type mRNA-treated mice were stimulated with single SLPs (Neo1, Neo3, and Neo4) that had shown IFN-γ production in the ELISpot assay (Fig. 5F). Gating strategies used for analysis are presented in Fig. S12. The results showed no significant differences in the percentage (Figs. S13A and S13B) or fold change (Fig. 6A) of the $CD3^+CD4^+IFN\text{-}\gamma^+$ population between splenocytes activated by mutant or wild-type mRNA treatment. However, significantly higher percentages were observed in the $CD3^+CD8^+IFN\text{-}\gamma^+$ population of mutant mRNA-treated splenocytes stimulated with mutant SLPs (Neo1, Neo3, and Neo4) compared to wild-type peptides (Figs. S13A and S13C). When normalized by the fold change of mutant-stimulated versus wild-type peptide stimulation, significantly higher fold changes were observed for Neo1 and Neo3 in mutant mRNA-treated mice compared to wild-type mRNA-treated mice, with only an increasing trend noted for Neo4 (Fig. 6B). These findings suggest that the mutant mRNA vaccine activates $CD8^+$ T cells to produce IFN-γ in a Neo1-, Neo3-, and Neo4-dependent manner.

To directly compare the safety and immune-activating ability of SLP and mRNA vaccines targeting identical neoantigens, we assessed body weight, histology, and blood

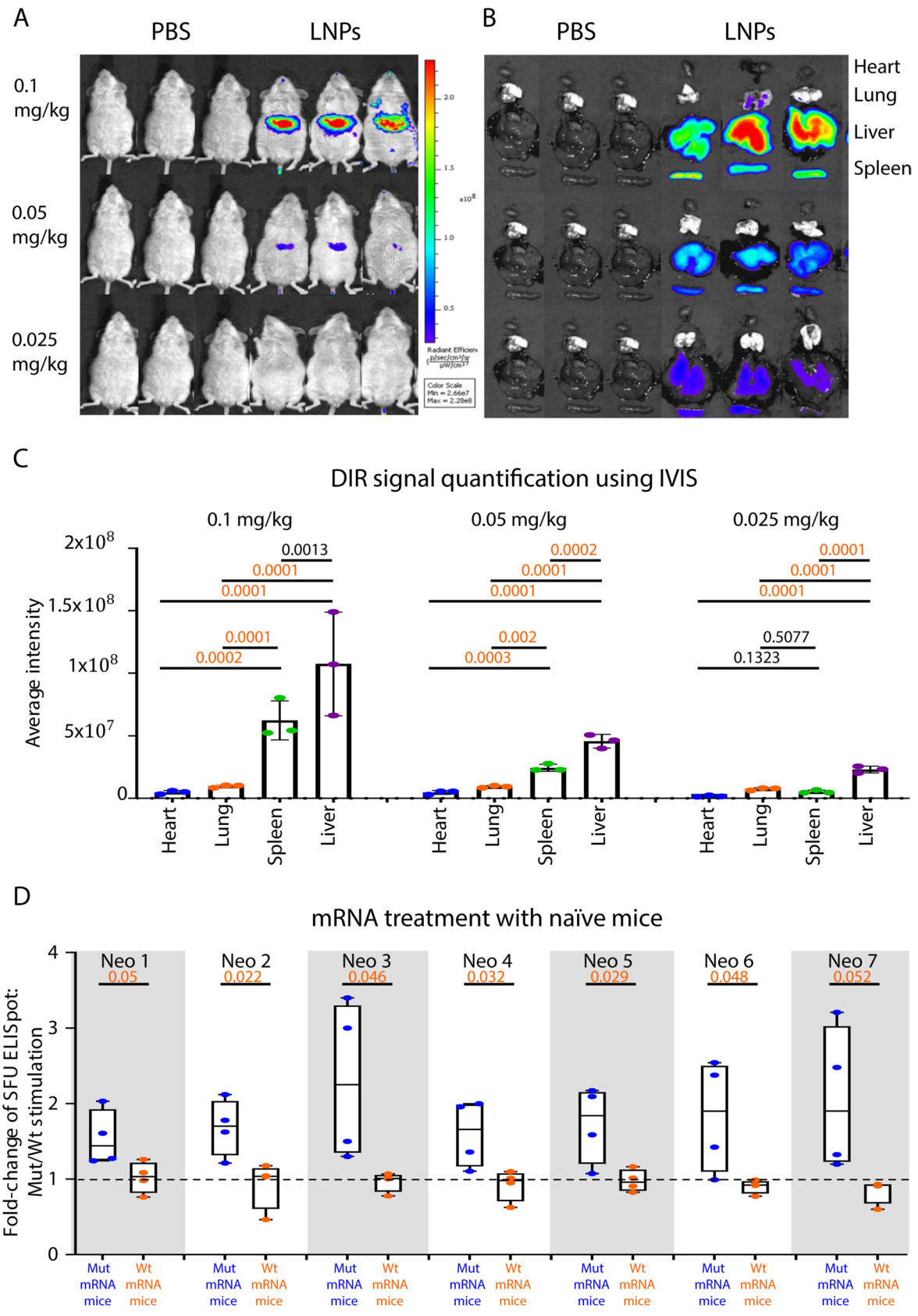
A
PBS
LNPs
0.1 mg/kg
0.05 mg/kg
0.025 mg/kg
B
PBS
LNPs
Heart
Lung
Liver
Spleen
C
DIR signal quantification using IVIS
0.1 mg/kg
0.05 mg/kg
0.025 mg/kg
Average intensity
2x10^8
1.5x10^8
1x10^8
5x10^7
0
0.0013
0.0001
0.0001
0.0001
0.0002
0.0002
0.0001
0.0001
0.0001
0.0003
0.002
0.0001
0.0001
0.0001
0.1323
0.5077
Heart
Lung
Spleen
Liver
D
mRNA treatment with naïve mice
Fold-change of SFU ELISpot: Mut/Wt stimulation
Neo 1
0.05
Neo 2
0.022
Neo 3
0.046
Neo 4
0.032
Neo 5
0.029
Neo 6
0.048
Neo 7
0.052
Mut mRNA mice
Wt mRNA mice

◂**Fig. 4** Distribution and specific induction of immune response by neo-mRNA in tumor-free mice injected with neo-mRNA-LNPs. **A** In vivo imaging to detect the distribution of neo-mRNA-LNPs in tumor-free mice injected with various doses of Neo-mRNA-LNPs. **B** In vivo imaging to detect the distribution of neo-mRNA-LNPs in heart, lung, liver and spleen of tumor-free mice injected with various doses of Neo-mRNA-LNPs. **C** DIR signal quantification of mRNA-LNPs in indicated organs of mice injected with mRNA-LNPs using the In Vivo Imaging System (IVIS). Each dot presents the signal from a mice, for each organs (heart, lung, spleen and liver). Mean ± SEM is shown. ns: not significant, $*p < 0.05$, $**p < 0.01$, $***p < 0.001$ (One-way ANOVA, Šídák's multiple comparisons test). **D** IFN-γ production was measured by ELISpot in splenocytes from naive mice after stimulation with wild-type (Wt) and mutant (Mut) peptides. Individual data point represents the fold change in the number of ELISpot spots in Mut peptide-activated splenocytes relative to the corresponding Wt-activated splenocytes for each individual mouse. Mean ± SEM is shown. ns: not significant, $*p < 0.05$, $**p < 0.01$, $***p < 0.001$ (independent (unpaired) two-sample t test)

hematology and biochemistry in mice vaccinated with either SLP or mRNA vaccines (Fig. S14). No significant differences were observed in safety profiles, including body weight and biochemical markers, between the two treatment groups. When evaluating tumor development, a clear distinction emerged between the two vaccine strategies. In the high TB model, all mice developed tumors, with no significant differences in therapeutic efficacy between the SLP- and mRNA-treated groups (Fig. S15A). However, in the low TB model, a striking difference was observed: all mice in the SLP group (4/4) developed tumors, whereas none of the mice vaccinated with mRNA developed tumors larger than 3000 mm^3. Fisher's Exact Test yielded a p-value of 0.0079, confirming a statistically significant difference between the two groups (Fig. S15A). Furthermore, mice treated with mutant mRNA exhibited significantly higher levels of IFN-γ compared to those treated with mutant SLPs when stimulated with Neo1, Neo3, and Neo4 peptides (Figs. S15B and S15C). These findings underscore the superior immunogenicity of mRNA vaccines in activating the immune response and preventing tumor development in the low TB model.

Splenocytes from neo-mRNA-vaccinated mice exhibit enhanced cytotoxic activity against LLC1 cells

To understand how the immune response of mRNA-vaccinated mice influenced tumor progression, we performed a cytotoxicity assay using splenocytes isolated from vaccinated mice and unpulsed LLC1 cells (Fig. S16A). We observed a dose-dependent trend of increased killing activity against unpulsed LLC1 cells when co-cultured with splenocytes from mutant mRNA-treated mice compared to those from wild-type mRNA-treated mice. This difference was statistically significant at the 5:1 and 10:1 ratios (Fig. S16B). These findings suggested that T cells from mutant mRNA-treated mice exhibited stronger cytotoxic activity against unpulsed LLC1 cells than those from wild-type mRNA-treated mice. This indicated that mRNA-LNPs activated the immune system in mice, potentially preventing tumor development in low TB mice.

To further validate our in vivo findings, we evaluated the cytotoxic activity of splenocytes harvested from neo-mRNA-vaccinated mice (effector cells) against LLC1 cells (target cells) pulsed with mutant peptides 1, 3 and 4, which elicited the strongest in vivo responses (Fig. 7A). At an effector-to-target ratio of 2:1, no differences in killing activity were observed between splenocytes from neo-mRNA and WT mRNA-vaccinated mice (Fig. 7B–D). At higher effector-to-target ratios of 5:1 and 10:1, we observed significantly enhanced cytotoxic activity against LLC1 cells when co-cultured with splenocytes from neo-mRNA-vaccinated mice, compared to those from WT mRNA-vaccinated mice, in the presence of mutant peptides 1, 3 and 4 (Fig. 7B–D). Consistent with the IFN-γ responses, these results suggest that the neo-mRNA vaccine can activate splenocytes to exert enhanced cytotoxicity toward neoantigens, particularly those derived from mutations 1, 3 and 4. Overall, our findings indicate that the neoantigen-based mRNA vaccine induces specific immune responses and anti-tumor immunity in mice with low TB, though these effects may be suppressed in high TB scenarios.

When directly comparing the cytotoxicity of splenocytes isolated from vaccinated mice in the low TB model, we consistently observed a statistically significant difference between the SLP and mRNA groups in their ability to kill peptide-pulsed LLC1 cells. Across all tested peptides, splenocytes from mRNA-vaccinated mice exhibited significantly higher cytotoxic activity against LLC1 cells than those from SLP-vaccinated mice (Fig. S17). These results, supported by rigorous statistical analysis, demonstrate the superior efficacy of the mRNA vaccine over the SLP vaccine in activating cytotoxic immune responses.

Discussions

Personalized neoantigen-based vaccination is promising in cancer immunotherapy for targeting multiple tumor-specific antigens. Researchers choose between two main delivery methods: SLPs and RNA-encoding tandem minigenes (TMGs), each with specific advantages for different tumors and patient profiles [21, 22]. However, no guidelines exist for selecting between these methods, complicating vaccine development. Our study aims to fill this gap by evaluating the safety and efficacy of SLP and TMG vaccines targeting the same neoantigens across different TB, providing insights to improve future cancer vaccine protocols. In this study,

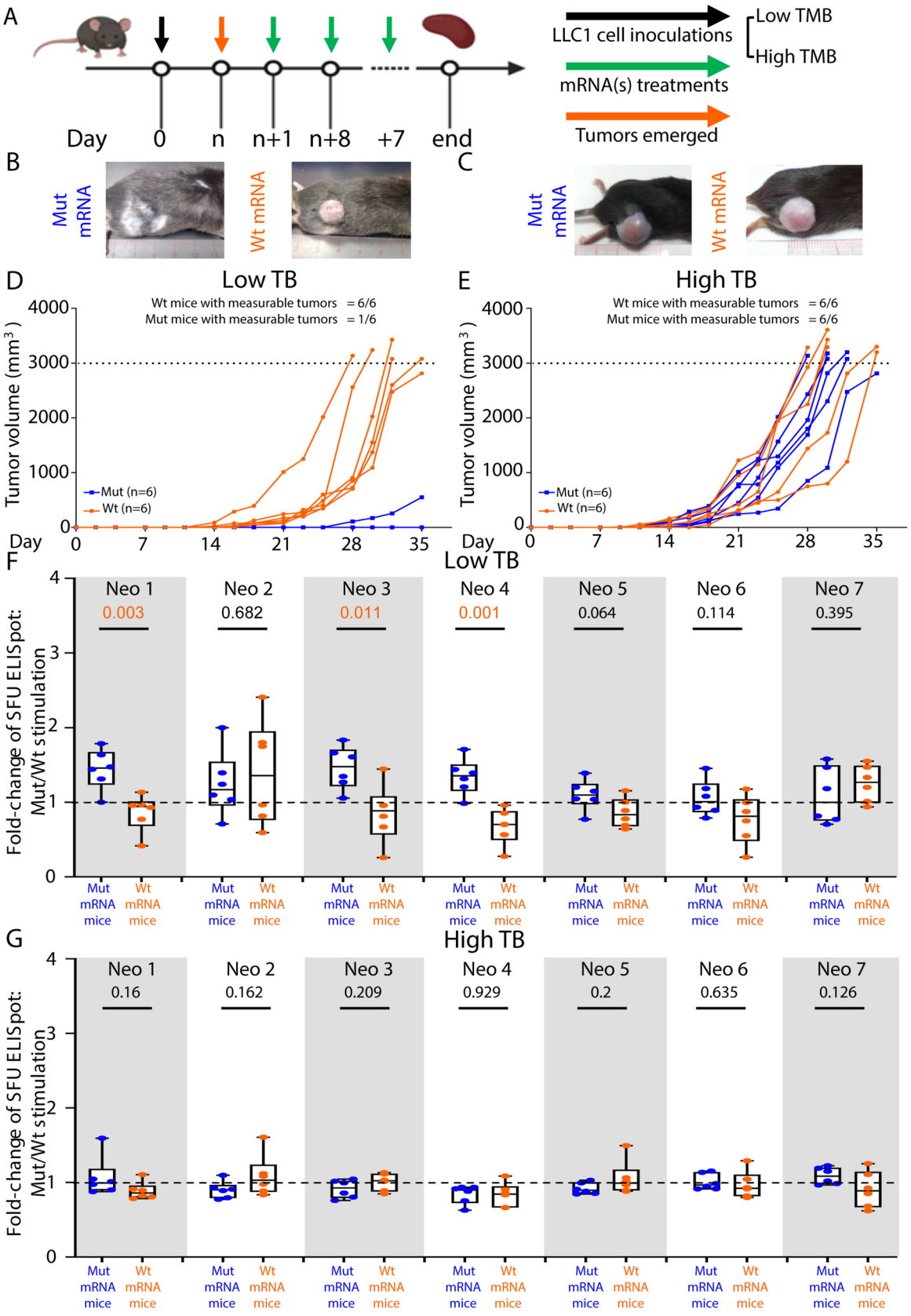
A
Day
0
n
n+1
n+8
+7
end
LLC1 cell inoculations
Low TMB
High TMB
mRNA(s) treatments
Tumors emerged
B
Mut mRNA
Wt mRNA
C
Mut mRNA
Wt mRNA
D
Low TB
Wt mice with measurable tumors = 6/6
Mut mice with measurable tumors = 1/6
Tumor volume (mm3)
Mut (n=6)
Wt (n=6)
Day
E
High TB
Wt mice with measurable tumors = 6/6
Mut mice with measurable tumors = 6/6
Tumor volume (mm3)
Mut (n=6)
Wt (n=6)
Day
F
Low TB
Neo 1 0.003
Neo 2 0.682
Neo 3 0.011
Neo 4 0.001
Neo 5 0.064
Neo 6 0.114
Neo 7 0.395
Fold-change of SFU ELISpot: Mut/Wt stimulation
Mut mRNA mice
Wt mRNA mice
G
High TB
Neo 1 0.16
Neo 2 0.162
Neo 3 0.209
Neo 4 0.929
Neo 5 0.2
Neo 6 0.635
Neo 7 0.126
Fold-change of SFU ELISpot: Mut/Wt stimulation
Mut mRNA mice
Wt mRNA mice

◂**Fig. 5** mRNA-LNP demonstrates anti-tumor activity in LLC syngeneic C57BL/6 mice with low TB. **A** Experimental design to test the therapeutic effect of mRNA vaccines on LLC-bearing C57BL/6 mice. **B**, **C** Representative images of tumors on day 30 under low (**B**) and high tumor budern (**C**). **D**, **E** Tumor development in LLC-bearing mice injected with wild-type or mutant mRNA vaccines under low (**D**) and high TB (**E**). **F**, **G** IFN-γ production was measured by ELISpot in splenocytes from vaccinated mice under low (**F**) and high TB (**G**) after stimulation with wild-type (Wt) and mutant (Mut) peptides. Individual data point represents the fold change in the number of ELISpot spots in Mut peptide-activated splenocytes relative to the corresponding Wt-activated splenocytes for each individual mouse. Mean ± SEM is shown. ns: not significant, $*p<0.05$, $**p<0.01$, $***p<0.001$ (independent (unpaired) two-sample t test)

TB refers to the number of cancer cells inoculated into the mice, while tumor mutation burden describes the number of mutations in the tumor's DNA. We aimed to evaluate the efficacy of the vaccines under low and high TB conditions.

We used the LLC mouse model, an aggressive, immunosuppressive model often employed in cancer research to study lung cancer and test immunotherapies under challenging conditions [23, 24]. The seven neoantigen candidates selected for this study were chosen based on their proven immunogenicity and relevance to LLC tumor (Fig. 1 and Table 1) [15], ensuring that our findings would be directly applicable to the development and implementation of neoantigen vaccines. A key observation in our study was that vaccinated tumor-bearing mice showed weak immune responses to the SLP-based vaccine (Fig. 2F–G), in contrast to the strong responses previously observed in tumor-naïve mice [25]. The difference likely stems from the tumor's immunosuppressive environment, leading to T cell exhaustion, altered antigen presentation, or immune tolerance to neoantigens [26]. In contrast, naïve mice, unaffected by these conditions, were able to mount a more effective immune response against the SLPs. We observed that some low TB mice responded to Mut SLP(s), while high TB mice showed no similar response (Fig. 2F). This difference may be due to the fact that T cells in the low TB model were not entirely suppressed and maintained a certain level of activation. Additionally, increasing the doses, adjusting schedules, and altering peptide components did not improve therapeutic outcomes (Fig. S5), confirming the ineffectiveness of the SLP approach for tumor vaccination under our testing conditions.

To improve tumor treatment beyond the SLP approach, we tested mRNA-based vaccines, which have several advantages: better antigen-presenting cell uptake, enhanced translation, and efficient HLA presentation [7, 27]. mRNA vaccines express multiple neoantigens, activating both CD8 + cytotoxic and CD4 + helper T cells for a stronger immune response, unlike peptide vaccines, which typically activate only one T cell type [28–30]. They also have an intrinsic adjuvant effect via toll-like receptor activation, avoiding the inconsistent responses seen with external adjuvants in peptide vaccines [31]. Lastly, mRNA vaccines offer prolonged antigen expression, unlike peptide vaccines, which degrade quickly and often need multiple boosters [32, 33]. To maximize the efficacy of mRNA vaccines in vivo, purifying the mRNA with HPLC and encapsulating it in LNPs is essential. This process removes dsRNA and truncated mRNA, minimizing unwanted immune responses [34]. LNPs also protect the mRNA and facilitate efficient delivery

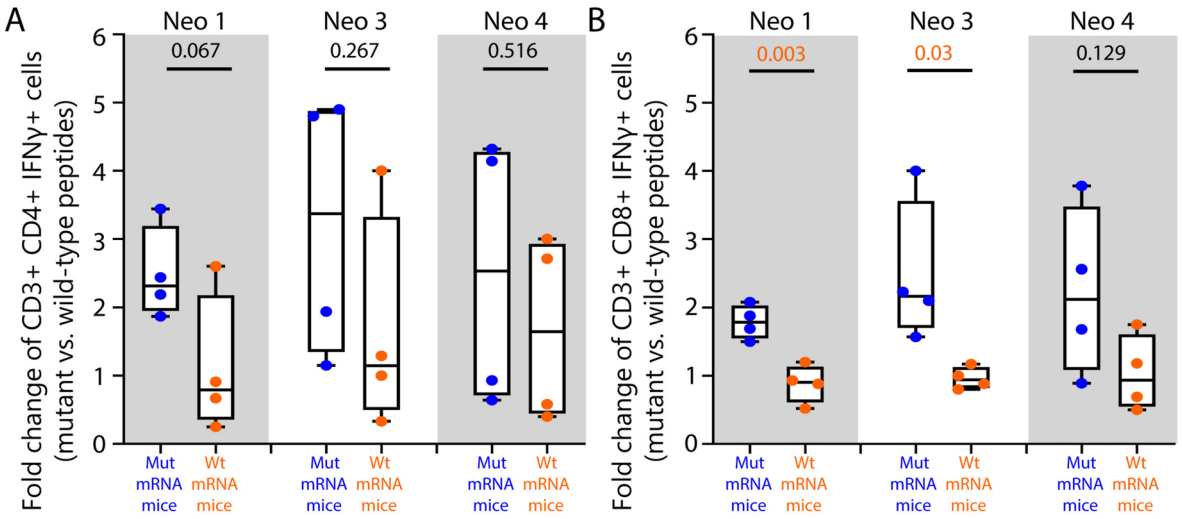

Fig. 6 Splenocytes from mice vaccinated with mRNA-LNPs activate CD8 + T cells to secrete IFN-γ when stimulated with SLPs. Fold change of CD3 + CD4 + IFNγ + cells (**A**) and CD3 + CD8 + IFNγ + cells (**B**) between mutant and wild-type peptides in mRNA-treated mice. Each dot represents the percentage of CD3 + CD4 + IFNγ + or CD3 + CD8 + IFNγ + cells after stimulation with SLP and subsequent ICS staining, derived from an individual vaccinated mouse. Data are presented as mean ± SEM. ns: not significant, $*p<0.05$, $**p<0.01$, $***p<0.001$ (independent, unpaired two-sample t test)

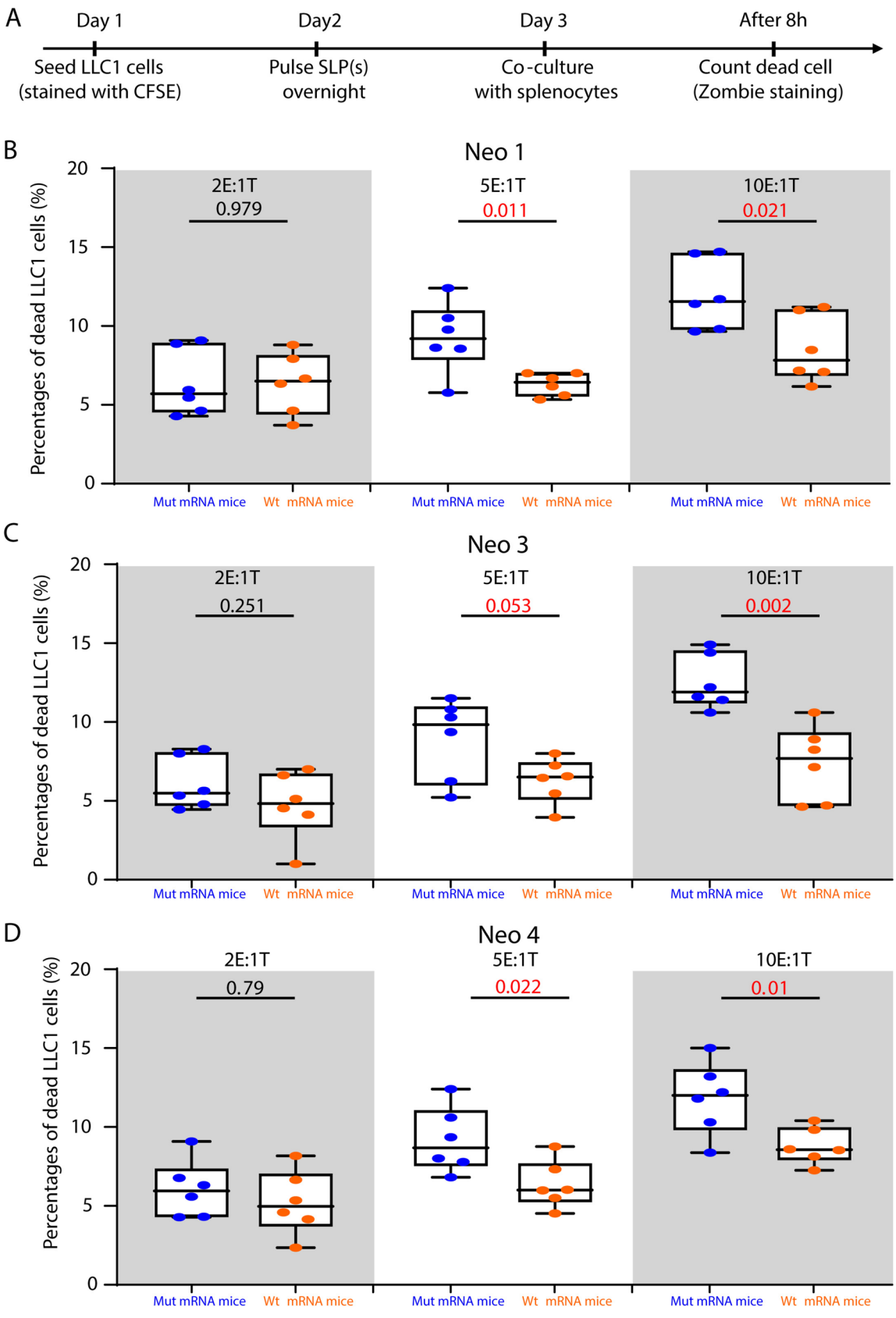
A
Day 1
Day2
Day 3
After 8h
Seed LLC1 cells (stained with CFSE)
Pulse SLP(s) overnight
Co-culture with splenocytes
Count dead cell (Zombie staining)
B
Neo 1
2E:1T
0.979
5E:1T
0.011
10E:1T
0.021
Percentages of dead LLC1 cells (%)
Mut mRNA mice
Wt mRNA mice
C
Neo 3
2E:1T
0.251
5E:1T
0.053
10E:1T
0.002
D
Neo 4
2E:1T
0.79
5E:1T
0.022
10E:1T
0.01

◂**Fig. 7** Splenocytes from mice vaccinated with mRNA-LNPs demonstrate cytotoxicity specifically against peptide-pulsed LLC1 cancer cells. **A** Experimental design for the cytotoxicity assay to quantify the cytotoxicity of splenocytes isolated from mRNA-LNP-vaccinated mice. **B**–**D** Percentage of dead LLC1 cells after stimulation with neoantigen candidate Neo 1 (**B**), Neo 3 (**C**) and Neo 4 (**D**) and co-culture with splenocytes from vaccinated LLC-bearing mice at specified ratios (2:1, 5:1 and 10:1). Each dot presents the percentage of dead LLC cell after culture with splenocyte from an individual vaccinated mouse. Mean ± SEM is shown. ns: not significant, $*p < 0.05$, $**p < 0.01$, $***p < 0.001$ (independent (unpaired) two-sample t test)

to cells [35]. Our current method for synthesizing LNPs has shown that we are able to eliminate a substantial amount of dsRNA prior to encapsulation. As a result, our LNPs contain predominantly single-stranded mRNA and exhibit uniform sizes (Fig. 3).

The IVIS results demonstrated that mRNA-LNPs successfully reached and accumulated in the lymphoid organs of naïve and tumor-bearing mice (Figs. 4, S7 and S8), consistent with findings that mRNA delivered via LNPs is transferred to the lymphoid system more efficiently compared to peptides [36]. At high doses, LNPs were detected near the tumors in mice (Fig S7). This enhanced uptake, along with specificity of mRNA-LNPs, makes them a more effective option for targeted cancer immunotherapy. The mRNA vaccine's safety was also thoroughly evaluated, showing non-serious inflammation in key organs like the liver and kidneys in all mice (Fig. S6). There were no significant differences in weight changes between the mRNA-vaccinated groups, and blood analyses of serum hematology and biochemistry showed only minimal variations. Furthermore, mice vaccinated with mRNA displayed no significant differences in weight changes, hematology, or blood biochemistry compared to those treated with SLPs (Fig. S14). These findings further support the potential of mRNA-based vaccines as a safe and effective option for neoantigen-based immunotherapy.

The mRNA vaccine showed strong immune activation in low TB mice (Figs. 5, S9, S11 and S16) but its effectiveness diminished in high TB mice (Figs. 5, S9 and S11). This phenomenon may be attributed to the immunosuppressive tumor microenvironment (TME), which can inhibit T cell activation or induce T cell exhaustion [37, 38]. Alternatively, altered antigen presentation due to high TB, as reported in a previous study, may enable tumors to evade immune detection through mechanisms such as MHC downregulation or upregulation of immune checkpoint ligands [39]. Therefore, adjustments in dosing schedules or combination therapy may be needed for high TB cases [40]. One low TB mouse in the Mut treatment group developed a small tumor, likely due to the loss of neoantigen [41], where the cell clone expressing the targeted neoantigen is eliminated while other surviving clones continue to proliferate.

RNA sequencing analysis confirmed that LLC cells express both wild-type and mutant allele transcripts for some neoantigens (Table 1). Peptide-MHC binding affinity was assessed as described [15], with a binding score below 3 indicating strong MHC binding (Table 1). However, due to negative selection in the thymus, T cells bearing TCRs with high affinity for wild-type peptides are likely eliminated during development [42, 43]. This process results in a peripheral TCR repertoire that predominantly consists of low-affinity TCRs for wild-type peptides, leading to reduced immunogenic responses. Consistent with this model, we propose that wild-type peptides predominantly induce baseline TCR activation, which corresponds with the low levels of IFN-γ production observed in PBMCs stimulated with wild-type peptides in vitro, as previously reported [15] and shown in Figs. S3C, S3D, S9C, and S9D. Not all seven neoantigen candidates elicited immune responses, despite being encoded in the same mRNA, raising questions about the factors influencing immunogenicity. Only three (Neo1, Neo3 and Neo4) showed significant differences compared to the Wt treatment group, as evidenced by an increased number of IFN-γ–secreting cells in ELISpot and ICS assays (Figs. 5, 6 and 7), indicating their neoantigen specificity. These variations may result from the neoantigens' inherent properties, presentation context, or immune regulatory mechanisms that suppress certain responses [44]. These findings suggest that specific mutations may enhance immunogenicity and could serve as promising candidates for vaccine development. Further research is needed to understand why some neoantigens fail to trigger an immune response, which could optimize neoantigen selection for future vaccines.

A direct comparison of the therapeutic efficacy of SLP and mRNA-LNP vaccines, with statistical assessment based on tumor development, survival rates, and immune system induction (measuring IFN-γ secretion and splenocyte cytotoxicity), demonstrated a higher efficacy of the mRNA-LNP vaccine under low TB conditions (Figs. S15 and S17). When considering these results alongside safety data (Fig. S14), we concluded that the mRNA-LNP vaccine is superior to the SLP vaccine in therapeutic effectiveness.

A significant limitation of our study is that we did not fully explore the mechanisms behind the differences in vaccine efficacy between low and high TB conditions. While neo-mRNA vaccination successfully induced strong neoantigen-specific immune responses and anti-tumor activity in mice with low TB, similar responses were lacking in those with high TB. This discrepancy raises several unresolved questions, as also noted in other research. First, we need to consider whether the increased tumor mutational burden (TB) and the tumor microenvironment (TME) work together to impair effective immune responses, potentially leading to T cell exhaustion due to chronic antigen exposure or antigen loss [45, 46]. Our study did not address potential T cell

dysfunction or changes in antigen presentation. Second, we must assess whether the differing immune responses result from variations in immune response dynamics between high and low TB conditions. If so, this may necessitate different dosing schedules for high TB mice [47]. Unfortunately, we did not explore these temporal aspects of immune activation. We recognize that peptide and mRNA vaccines differ fundamentally, each with inherent limitations. Our approach seeks to optimize the efficacy of both vaccine types while ensuring their evaluation reflects real-world conditions. This methodology aligns with established best practices in the field, as highlighted in recent reviews [48, 49]. Moving forward, we aim to further enhance mRNA vaccine efficacy by refining LNP formulations and optimizing vaccination strategies. Therefore, further research is essential to delineate the specific mechanisms that limit the effectiveness of neoantigen-based vaccines in high TB settings. Understanding these mechanisms could help inform strategies to overcome immune resistance and improve vaccine efficacy in more advanced stages of cancer.

Supplementary Information The online version contains supplementary material available at https://doi.org/10.1007/s00262-025-03992-7.

Acknowledgements We thank Dr. Kien Nguyen for proofreading our manuscript. We thank Dr. Nghia Truong Phuoc for assistance with the LNP encapsulation protocol (https://research.monash.edu/en/persons/nghia-truong-Phuoc).

Author contributions Cao Minh Nguyen, Trung T. Vu, Minh Nguyen Nguyen, and Thao-Suong Tran-Nguyen performed cancer cell and vaccine injections, conducted downstream in vitro analyses, and were responsible for formal analysis, data curation, methodology development, and experiments. Chi Thien Huynh and Quang Thanh Ha managed mouse husbandry and monitoring, including tumor measurement, weighing, feeding, and sample collection at the endpoint. Hoai Nghia Nguyen provided supervision and guidance on conceptualization, while Cao Minh Nguyen and Le Son Tran contributed to conceptualization and manuscript writing. All authors read and approved the final manuscript.

Funding This research was funded by a NexCalibur Therapeutic grant (NC01). Le Son Tran holds the equity in NexCalibur Therapeutic.

Data availability No datasets were generated or analyzed during the current study.

Declarations

Conflict of interest The authors declare no competing interests.

Ethical approval Animal experimentation was approved by the Animal Ethics Committee A at the University of Science in Ho Chi Minh City, Vietnam (permit number 562/KHTN-ACUCUS), and mice were euthanized via CO2 inhalation.

Open Access This article is licensed under a Creative Commons Attribution-NonCommercial-NoDerivatives 4.0 International License, which permits any non-commercial use, sharing, distribution and reproduction in any medium or format, as long as you give appropriate credit to the original author(s) and the source, provide a link to the Creative Commons licence, and indicate if you modified the licensed material. You do not have permission under this licence to share adapted material derived from this article or parts of it. The images or other third party material in this article are included in the article's Creative Commons licence, unless indicated otherwise in a credit line to the material. If material is not included in the article's Creative Commons licence and your intended use is not permitted by statutory regulation or exceeds the permitted use, you will need to obtain permission directly from the copyright holder. To view a copy of this licence, visit http://creativecommons.org/licenses/by-nc-nd/4.0/.

References

1. Janelle V, Rulleau C, Del Testa S, Carli C, Delisle JS (2020) T-cell immunotherapies targeting histocompatibility and tumor antigens in hematological malignancies. Front Immunol 11:276
2. Fan T et al (2023) Therapeutic cancer vaccines: advancements, challenges, and prospects. Signal Transduct Target Ther 8:450
3. Buonaguro L, Tagliamonte M (2023) Peptide-based vaccine for cancer therapies. Front Immunol 14:1210044
4. Liu D et al (2024) Advancements and challenges in peptide-based cancer vaccination: a multidisciplinary perspective. Vaccines (Basel) 12:950
5. Wang B, Pei J, Xu S, Liu J, Yu J (2023) Recent advances in mRNA cancer vaccines: meeting challenges and embracing opportunities. Front Immunol 14:1246682
6. Thundimadathil J (2012) Cancer treatment using peptides: current therapies and future prospects. J Amino Acids 2012:967347
7. Li Y et al (2023) mRNA vaccine in cancer therapy: current advance and future outlook. Clin Transl Med 13:e1384
8. Biswas N, Chakrabarti S, Padul V, Jones LD, Ashili S (2023) Designing neoantigen cancer vaccines, trials, and outcomes. Front Immunol 14:1105420
9. Cafri G et al (2020) mRNA vaccine-induced neoantigen-specific T cell immunity in patients with gastrointestinal cancer. J Clin Invest 130:5976–5988
10. Rabinovich GA, Gabrilovich D, Sotomayor EM (2007) Immunosuppressive strategies that are mediated by tumor cells. Annu Rev Immunol 25:267–296
11. Xiang Y et al (2024) Mechanisms of resistance to targeted therapy and immunotherapy in non-small cell lung cancer: promising strategies to overcoming challenges. Front Immunol 15:1366260
12. Feng Y et al (2022) IL-9 stimulates an anti-tumor immune response and facilitates immune checkpoint blockade in the CMT167 mouse model. Lung Cancer 174:14–26
13. Johnson AM et al (2020) Cancer cell-intrinsic expression of MHC class II regulates the immune microenvironment and response to anti-PD-1 therapy in lung adenocarcinoma. J Immunol 204:2295–2307
14. Ha TY (2009) The role of regulatory T cells in cancer. Immune Netw 9:209–235
15. Chen T et al (2020) Comprehensive mutanome analysis of Lewis lung cancer reveals immunogenic neoantigens for therapeutic vaccines. Biochem Biophys Res Commun 525:607–613
16. Kariko K, Muramatsu H, Ludwig J, Weissman D (2011) Generating the optimal mRNA for therapy: HPLC purification eliminates immune activation and improves translation of nucleoside-modified, protein-encoding mRNA. Nucleic Acids Res 39:e142
17. McKenzie RE, Minnell JJ, Ganley M, Painter GF, Draper SL (2023) mRNA synthesis and encapsulation in ionizable lipid nanoparticles. Curr Protoc 3:e898
18. Rossino G et al (2023) Peptides as therapeutic agents: challenges and opportunities in the green transition era. Molecules 28:7165

19. Weber JS et al (2024) Individualised neoantigen therapy mRNA-4157 (V940) plus pembrolizumab versus pembrolizumab monotherapy in resected melanoma (KEYNOTE-942): a randomised, phase 2b study. Lancet 403:632–644
20. Li M et al (2022) The nano delivery systems and applications of mRNA. Eur J Med Chem 227:113910
21. Malla R, Srilatha M, Farran B, Nagaraju GP (2024) mRNA vaccines and their delivery strategies: a journey from infectious diseases to cancer. Mol Ther 32:13–31
22. Sasada T, Noguchi M, Yamada A, Itoh K (2012) Personalized peptide vaccination: a novel immunotherapeutic approach for advanced cancer. Hum Vaccin Immunother 8:1309–1313
23. He Q, Sun C, Pan Y (2024) Whole-exome sequencing reveals Lewis lung carcinoma is a hypermutated Kras/Nras-mutant cancer with extensive regional mutation clusters in its genome. Sci Rep 14:100
24. Janker F, Weder W, Jang JH, Jungraithmayr W (2018) Preclinical, non-genetic models of lung adenocarcinoma: a comparative survey. Oncotarget 9:30527–30538
25. Hailemichael Y et al (2013) Persistent antigen at vaccination sites induces tumor-specific CD8(+) T cell sequestration, dysfunction and deletion. Nat Med 19:465–472
26. Xia A, Zhang Y, Xu J, Yin T, Lu XJ (2019) T Cell Dysfunction in Cancer Immunity and Immunotherapy. Front Immunol 10:1719
27. Gote V et al (2023) A comprehensive review of mRNA vaccines. Int J Mol Sci 24:2700
28. Kunzli M et al (2022) Route of self-amplifying mRNA vaccination modulates the establishment of pulmonary resident memory CD8 and CD4 T cells. Sci Immunol 7:eadd3075
29. Harao M, Mittendorf EA, Radvanyi LG (2015) Peptide-based vaccination and induction of CD8+ T-cell responses against tumor antigens in breast cancer. BioDrugs 29:15–30
30. Huff AL et al (2023) CD4 T cell-activating neoantigens enhance personalized cancer vaccine efficacy. JCI Insight. https://doi.org/10.1172/jci.insight.174027
31. Petkar KC et al (2021) An overview of nanocarrier-based adjuvants for vaccine delivery. Pharmaceutics 13:455
32. Huang T et al (2022) Lipid nanoparticle-based mRNA vaccines in cancers: current advances and future prospects. Front Immunol 13:922301
33. Wang YS et al (2023) mRNA-based vaccines and therapeutics: an in-depth survey of current and upcoming clinical applications. J Biomed Sci 30:84
34. Kwon S, Kwon M, Im S, Lee K, Lee H (2022) mRNA vaccines: the most recent clinical applications of synthetic mRNA. Arch Pharm Res 45:245–262
35. Esprit A et al (2020) Neo-Antigen mRNA Vaccines. Vaccines (Basel) 8:776
36. Liu Y et al (2024) Development of mRNA lipid nanoparticles: targeting and therapeutic aspects. Int J Mol Sci 25:10166
37. Jiang W et al (2020) Exhausted CD8+T cells in the tumor immune microenvironment: new pathways to therapy. Front Immunol 11:622509
38. Lopresti L, Tatangelo V, Baldari CT, Patrussi L (2024) Rewiring the T cell-suppressive cytokine landscape of the tumor microenvironment: a new frontier for precision anti-cancer therapy. Front Immunol 15:1418527
39. Cornel AM, Mimpen IL, Nierkens S (2020) MHC class I downregulation in cancer: underlying mechanisms and potential targets for cancer immunotherapy. Cancers (Basel) 12:1760
40. Donhauser LV et al (2023) Responses of patients with cancer to mRNA vaccines depend on the time interval between vaccination and last treatment. J Immunother Cancer 11:e007387
41. Wang Y, Xu J, Lan T, Zhou C, Liu P (2023) The loss of neoantigens is an important reason for immune escape in multiple myeloma patients with high intratumor heterogeneity. Cancer Med 12:21651–21665
42. Klein L, Kyewski B, Allen PM, Hogquist KA (2014) Positive and negative selection of the T cell repertoire: what thymocytes see (and don't see). Nat Rev Immunol 14:377–391
43. Madley R et al (2020) Negative selection of human T cells recognizing a naturally-expressed tissue-restricted antigen in the human thymus. J Transl Autoimmun 3:100061
44. Xie N et al (2023) Neoantigens: promising targets for cancer therapy. Signal Transduct Target Ther 8:9
45. Jhunjhunwala S, Hammer C, Delamarre L (2021) Antigen presentation in cancer: insights into tumour immunogenicity and immune evasion. Nat Rev Cancer 21:298–312
46. Chow A, Perica K, Klebanoff CA, Wolchok JD (2022) Clinical implications of T cell exhaustion for cancer immunotherapy. Nat Rev Clin Oncol 19:775–790
47. Maleki Vareki S (2018) High and low mutational burden tumors versus immunologically hot and cold tumors and response to immune checkpoint inhibitors. J Immunother Cancer 6:157
48. Hou X, Zaks T, Langer R, Dong Y (2021) Lipid nanoparticles for mRNA delivery. Nat Rev Mater 6:1078–1094
49. Song K, Pun SH (2024) Design and evaluation of synthetic delivery formulations for peptide-based cancer vaccines. BME Front 5:0038

Publisher's Note Springer Nature remains neutral with regard to jurisdictional claims in published maps and institutional affiliations.